

distribution function  $g(\Delta)$ , which might, for example, be Gaussian when

$$g(\Delta) = (\pi\alpha^2)^{-1/2} \exp(-\Delta^2/\alpha^2).$$

As  $N$  tends to infinity all possible configurations will be assumed during the aggregation process. The general term in the series of (10) is

$$G^n(q) \exp(-q^2 \rho_n^2) \cos(qnd),$$

which approximates to

$$\exp\{-q^2[(n\alpha^2/4) + \rho_n^2]\} \cos(qnd)$$

if  $g(\Delta)$  is Gaussian. Note that  $d$  is only defined for disorder of the second kind (as in § 5) if

$$\langle \Delta_n \rangle = 0.$$

This condition is essentially a description of a disordered model of the kind we are investigating, *i.e.* one in which all possible 'atomic' configurations are assumed.

#### References

- BLASIE, J. K. & WORTHINGTON, C. R. (1969). *J. Mol. Biol.* **39**, 417–439.
- BLAUROCK, A. E. & NELANDER, J. C. (1976). *J. Mol. Biol.* **103**, 421–431.
- BORN, M. (1942). *Proc. R. Soc. London Ser. A*, **180**, 397–413.
- BORN, M. & VON KARMAN, T. (1912). *Phys. Z.* **13**, 297–309.
- COX, R. W., GRANT, R. A. & HORNE, R. W. (1967). *J. R. Microscop. Soc.* **87**, 123–142.
- ENDERBY, J. E. (1972). *Adv. Struct. Res. Diffraction Methods*, **4**, 65–104.
- GUGGENHEIM, E. A. (1959). *Boltzmann's Distribution Law*, pp. 37–41. Amsterdam: North-Holland.
- HOSEMANN, R. (1951). *Acta Cryst.* **4**, 520–530.
- HOSEMANN, R. (1973). *Endeavour*, **32**, 99–105.
- HOSEMANN, R. & BAGCHI, S. N. (1962). *Direct Analysis of Diffraction by Matter*. Amsterdam: North-Holland.
- HOSEMANN, R., DREISSIG, W. & NEMETSCHKE, T. (1974). *J. Mol. Biol.* **83**, 275–280.
- HUKINS, D. W. L. (1978). *J. Theor. Biol.* **71**, 661–667.
- HUKINS, D. W. L. & WOODHEAD-GALLOWAY, J. (1977). *Mol. Cryst. Liq. Cryst.* **41**, 33–39.
- HUKINS, D. W. L. & WOODHEAD-GALLOWAY, J. (1978). *Biochem. Soc. Trans.* **6**, 238–239.
- HYBL, A. (1976). *Mol. Cryst. Liq. Cryst.* **36**, 271–278.
- HYBL, A. (1977). *J. Appl. Cryst.* **10**, 141–146.
- LANGRIDGE, R., WILSON, H. R., HOOPER, C. W., WILKINS, M. H. F. & HAMILTON, L. D. (1960). *J. Mol. Biol.* **2**, 19–37.
- LEBOWITZ, J. L. & PERCUS, J. (1966). *Phys. Rev.* **144**, 251–258.
- MILLER, A. (1976). In *Biochemistry of Collagen*, edited by G. N. RAMACHANDRAN & A. H. REDDI, pp. 85–136. New York and London: Plenum.
- NELANDER, J. C. & BLAUROCK, A. E. (1978). *J. Mol. Biol.* **118**, 497–532.
- O'BRIEN, E. J., GILLIS, J. M. & COUCH, J. (1975). *J. Mol. Biol.* **99**, 461–475.
- ORNSTEIN, L. S. & ZERNICKE, F. (1914). *Proc. Acad. Sci. Amsterdam*, **17**, 793.
- PRINS, J. A. (1931). *Z. Physik.* **71**, 445–449.
- SALPETRE, E. E. (1958). *Ann. Phys. (NY)*, **5**, 183–223.
- STEWART, M. & MCLACHLAN, A. D. (1976). *J. Mol. Biol.* **103**, 251–269.
- THIELE, E. (1963). *J. Chem. Phys.* **39**, 474–479.
- WERTHEIM, M. S. (1963). *Phys. Rev. Lett.* **10**, 321–323.
- WHEELER, E. J. & LEWIS, D. (1977). *Calcif. Tissue Res.* **24**, 243–248.
- WILLIAMS, R. J. P. (1977). *Nature (London)*, **266**, 481.
- WOODHEAD-GALLOWAY, J., GASKELL, T. & MARCH, N. H. (1968). *J. Phys. C*, **1**, 271–285.
- WOODHEAD-GALLOWAY, J., HUKINS, D. W. L., KNIGHT, D. P., MACHIN, P. A. & WEISS, J. B. (1978). *J. Mol. Biol.* **118**, 567–578.
- WOODHEAD-GALLOWAY, J. & MACHIN, P. A. (1976a). *Acta Cryst.* **A32**, 368–372.
- WOODHEAD-GALLOWAY, J. & MACHIN, P. A. (1976b). *Mol. Phys.* **32**, 41–48.
- WOODHEAD-GALLOWAY, J. & YOUNG, W. H. (1978). *Acta Cryst.* **A34**, 12–18.

*Acta Cryst.* (1980). **A36**, 205–210

## The Electron-Density Distribution in Silicon

BY C. SCHERINGER

*Institut für Mineralogie der Universität Marburg, D 3550 Marburg/Lahn, Federal Republic of Germany*

(Received 25 July 1979; accepted 11 September 1979)

#### Abstract

The electron-density distribution in crystalline silicon was refined with a three-parameter density model which was originally designed by Brill. The same data sets

were used as by other authors [Price, Maslen & Mair (PMM) (1978). *Acta Cryst.* **A34**, 183–193; Hansen & Coppens (1978). *Acta Cryst.* **A34**, 909–921] in refining their multipole models. The data sets are (1) the 15 Mo  $K\alpha$  room-temperature data of Aldred & Hart

(AH) [*Proc. R. Soc. London Ser. A* (1973), **322**, 223–238, 239–254], (2) the 15 AH data plus the 222 and 442 data of Roberto & Batterman [*Phys. Rev. B* (1970), **2**, 3220–3226] and Trucano & Batterman [*Phys. Rev. B* (1972), **6**, 3659–3666], respectively, (3) the 17 data of (2) plus four data measured by Hattori, Kuriyama, Katagawa & Kato (HKKK) [*J. Phys. Soc. Jpn* (1965), **20**, 988–996].  $R$  for these data sets, obtained with the present density model, is 0.12, 0.13 and 0.30%, respectively. This compares well with the values obtained by the other authors with their multipole models. In the deformation density, PMM found a Si–Si bond peak of height  $0.13 \text{ e } \text{Å}^{-3}$  with data set (1), whereas Yang & Coppens [*Solid State Commun.* (1974), **15**, 1555–1559] found a peak height of  $0.29 \text{ e } \text{Å}^{-3}$  with data set (3). With data set (2) a peak height of  $0.20 \text{ e } \text{Å}^{-3}$  is found in agreement with the result of PMM. However, the increase of the peak height to  $0.29 \text{ e } \text{Å}^{-3}$  with data set (3) is an inaccuracy which arises from the fact that the four HKKK reflections were not measured accurately enough.

### Introduction

The electron-density distribution in crystalline silicon has been studied extensively, mainly by Göttlicher & Wölfel (1959); De Marco & Weiss (1965); Hattori, Kuriyama, Katagawa & Kato (1965, hereafter referred to as HKKK); Dawson (1967, 1975); McConnell & Sanger (1970); Aldred & Hart (1973, hereafter referred to as AH); Yang & Coppens (1974, hereafter referred to as YC); Hansen & Coppens (1978, hereafter referred to as HC); Price, Maslen & Mair (1978, hereafter referred to as PMM). Two X-ray data sets were obtained by *Pendellösung*-fringe measurements on perfect crystals, one by HKKK, the other by AH. AH's data represent the most accurate X-ray data ever measured on a crystal.

The high accuracy of AH's data led us to examine a density model which was originally proposed by Brill (1959, 1960) in his investigation of diamond, and which we have applied in a somewhat refined form to decaborane and cyanuric acid (Dietrich & Scheringer, 1978, 1979). An examination of this type of model is particularly interesting in view of the refinements that have been performed with multipole density models by PMM and HC; also with AH's data. The density model according to Brill consists of atomic cores and Gaussian-distributed charge clouds which are placed in the centre of the bonds. Thus, this model allows an expedient description of the accumulation of charge in covalent bonds. HKKK also used this model for the interpretation of their X-ray data on silicon, but the quality of their data did not appear to be sufficient to examine the usefulness of the model as such.

A factual problem arises through the study of the deformation densities for silicon which have been

published. With the 15 data of AH, PMM found a bond peak of height  $0.13 \text{ e } \text{Å}^{-3}$ , whereas YC, with the inclusion of the 222 reflection (Roberto & Batterman, 1970) and the 442 reflection (Trucano & Batterman, 1972) and four reflections of HKKK, found a peak of height  $0.29 \text{ e } \text{Å}^{-3}$ . We recalculated the maps\* (PMM's map with the  $F_o$ 's instead of the  $F_c$ 's) and, moreover, calculated a map with the 15 data of AH and the 222, 442 reflections, and found a peak height of  $0.20 \text{ e } \text{Å}^{-3}$  (Fig. 1). The 222 reflection strongly contributes to the bond density ( $0.07 \text{ e } \text{Å}^{-3}$ ), the very weak 442 reflection hardly at all. Thus, the difference of  $0.09 \text{ e } \text{Å}^{-3}$  to the result of YC ( $0.29 \text{ e } \text{Å}^{-3}$ ) has to be attributed to the four HKKK reflections in the Fourier map. Here the question arises why these four reflections have such a large effect on the bond density. Two explanations suggest themselves: series termination error or errors in the measured intensities. The study of this problem is the second purpose of this paper.

Firstly, we describe the treatment of the data, discuss the parameters and the structure factor for our density model and present the results of the refinement. Then we shall compare  $R$  values and goodness-of-fit values of our model with those reported in the literature. Finally, we shall investigate the discrepancy found in the deformation densities.

### Refinement of the density model

The observed structure factors are the 15 Mo  $K\alpha$  room-temperature data from AH's Table 3, plus six data

\* The Fourier syntheses were computed with the program written by Finger & Prince (1975).

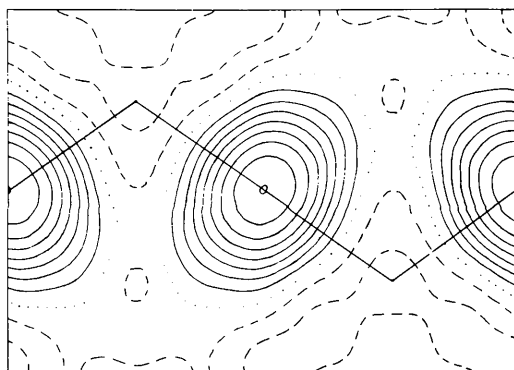


Fig. 1. Deformation density along the Si–Si bond ( $xxz$  section). The density was calculated with coefficients  $F_o - F_c$  (free-atom model) from data set 17 of Table 1 and with signs of column  $F_c$  (bond). Contour interval:  $0.025 \text{ e } \text{Å}^{-3}$ . Positive density: full lines; zero density: dotted; negative density: dashed.

from other authors, Table 1. The data were corrected for anomalous absorption by the method of YC, with  $f' = 0.1003$  and  $f'' = 0.07117$  (Wagenfeld, Kühn & Guttman, 1973). The weights were calculated as  $w = 1/\sigma^2$  with the  $\sigma(F)$  as given by YC. For the reflections 111 and 442, however, a larger  $\sigma(F)$  was used,  $\sigma(F) = 0.020$ , to avoid the refinement being based mainly on these two reflections.

The model for the density distribution consists of a spherically symmetric atomic core with a positive net charge  $q(\text{Si})$ , and negative Gaussian-distributed charges at the bond centres,  $q(\text{bond})$ . Neutrality in the crystal demands

$$q(\text{Si}) + 2q(\text{bond}) = 0. \quad (1)$$

The smearing tensor for the bond charges has only two independent components (site symmetry  $\bar{3}$ ); we put  $V_{11} = V_{22}$  perpendicular to and  $V_{33}$  along the bond. Along the bond we assume that the bond charges vibrate like the Si cores, but perpendicular to the bond we assume smaller vibrations (Scheringer, 1977). With an assessment of Fujimoto (1974), we reduce the vibration components of the bond charges perpendicular to the bond by a factor of  $\eta = 0.74$ . Thus our model contains only three density parameters,  $q(\text{Si})$ ,  $V_{11}$  and  $V_{33}$ , and an isotropic vibration parameter  $B$ . With these para-

meters and Si located at  $\frac{1}{8}, \frac{1}{8}, \frac{1}{8}$ , the structure factor for the face-centered cell is given by

$$\begin{aligned} F(hkl) = & 8f(\text{Si}) \cos[\pi(h+k+l)/4] \\ & \times \exp[-B(\sin^2 \theta) \lambda^{-2}] + 4q(\text{bond}) \\ & \times \exp\{-(h^2 + k^2 + l^2)/3a^2 [2\pi^2(2V_{11} + V_{33}) \\ & + B(1 + 2\eta)/4]\} \sum_{j=1}^4 \cos[2\pi(hx_j + ky_j + lz_j)] \\ & \times \exp\{-2(h_j k_j + h_j l_j + k_j l_j)/3a^2 \\ & \times [2\pi^2(V_{33} - V_{11}) + B(1 - \eta)/4]\}, \quad \eta = 0.74. \quad (2) \end{aligned}$$

The sum over  $j$  goes over the four symmetry-equivalent positions of the bond charges (centres of the Si-Si bonds).  $h_j, k_j, l_j$  may differ only in sign for the four values of  $j$ ; the signs can be obtained from the symmetry transformations of the second-order tensors (Scheringer, 1979).

The scattering factor  $f(\text{Si})$  is set up as the sum of the scattering factor for the  $\text{Si}^{4+}$  core,  $f(\text{Si}^{4+})$ , and the scattering factor for the valence shell,  $f_{\text{val}}$ . The latter is calculated as the difference  $f(\text{Si}^0) - f(\text{Si}^{4+})$ , with one modification. The grid points for these two scattering curves are taken from *International Tables for X-ray Crystallography* (1974), and for each reflection a linear interpolation in  $\sin \theta/\lambda$  is carried out. Concerning the detailed shape of the valence shell, we have taken over an idea from Coppens (1977); see also HC and Coppens *et al.* (1979). These authors found that the valence shell contracts with a positive net charge of the atom and expands with a negative net charge. To describe this change in shape, they introduced a contraction/expansion parameter  $\kappa$  along with the population parameter. In this work we apply only one parameter, the net charge  $q(\text{Si})$  (then the population is given by  $P = 4 - q$ ), and use it to steer the contraction/expansion of the valence shell. Here, we use a mathematical formalism which differs from that of Coppens (1977) and is simpler to apply in computation. We choose an exponential factor of  $f_{\text{val}}$ , and then write for  $f(\text{Si})$  in (2)

$$\begin{aligned} f(\text{Si}) = & f(\text{Si}^{4+}) + (1 - q/4)[f(\text{Si}^0) - f(\text{Si}^{4+})] \\ & \times \exp[C_1(q + C_2) \sin \theta/\lambda], \quad (3) \end{aligned}$$

where  $C_1$  and  $C_2$  are positive constants. The density distribution corresponding to (3) can be calculated analytically only for the case of the expansion,  $q + C_2 < 0$ . Here it is the convolution of  $\rho_{\text{val}}$  with the inverse Fourier transform of the exponential factor. With  $(1/2)C_1|q + C_2| \equiv \alpha$ , this is known to be  $8\pi\alpha[\alpha^2 + (2\pi r)^2]^{-2}$  (Hirshfeld, 1971). For contraction of the valence shell ( $q + C_2 > 0$ ), the inverse Fourier transform of the exponential factor does not exist, but we can show that the inverse Fourier transform of  $f(\text{Si})$  does. Here we have to show that  $f(\text{Si})$  converges towards zero for  $\sin \theta/\lambda \rightarrow \infty$ . In this context we refer

Table 1. *Observed and calculated structure factors for Si per face-centred cell*

The observed structure factors are derived from the experimental structure factors listed by YC (Table 1), by applying the correction for anomalous dispersion for *Pendellösung* fringe data ( $f' = 0.1003$ ,  $f'' = 0.07117$ ).  $F_o(\text{bond}) = F_c$  calculated from the bonding model used in this work;  $F_o(\text{FAM}) = F_c$  calculated from the free-atom model with  $B = 0.4700$ . RB refers to Roberto & Batterman (1970), TB to Trucano & Batterman (1972).

$hkl$	$F_o(\sigma[F_o])$	$F_c(\text{bond})$	$F_c(\text{FAM})$	Reference
1 1 1	59.967 (4)	-59.994	-58.900	AH
2 2 0	67.070 (48)	-67.141	-67.542	AH
3 1 1	43.421 (40)	-43.392	-44.237	AH
2 2 2	1.442 (40)	1.419	0.0	RB
4 0 0	55.873 (80)	-55.828	-56.399	AH
3 3 1	38.008 (40)	38.026	37.701	AH
4 2 2	48.935 (72)	48.890	48.774	AH
3 3 3	32.677 (40)	32.785	32.744	AH
5 1 1	32.721 (40)	32.731	32.744	AH
4 4 0	42.592 (32)	42.625	42.551	AH
5 3 1	28.912 (408)	28.654	28.628	HKKK
4 4 2	0.034 (2)	0.025	0.0	TB
6 2 0	37.005 (524)	37.307	37.321	HKKK
5 3 3	24.921 (352)	-25.126	-25.157	HKKK
4 4 4	32.948 (40)	-32.872	-32.909	AH
5 5 1	22.717 (324)	-22.207	-22.227	HKKK
6 4 2	29.216 (56)	-29.139	-29.165	AH
6 6 0	23.297 (56)	-23.254	-23.267	AH
5 5 5	15.783 (40)	15.797	15.805	AH
8 4 4	17.139 (48)	17.205	17.205	AH
8 8 0	12.234 (64)	12.216	12.210	AH

to the fact that the scattering factors of the atoms and ions can be represented very well by a sum of Gaussian functions in  $\sin \theta/\lambda$  (*International Tables for X-ray Crystallography*, 1974). Hence, the scattering curves converge faster to zero than the exponential factor to infinity. Since we calculate the density distribution by a Fourier series, the lack of knowledge concerning the inverse Fourier transform of  $f(\text{Si})$  as given by (3) causes no harm. Numerical values for  $C_1$  and  $C_2$  are estimated from the results of Coppens *et al.* (1979) for the C and N atoms, and from the position and slope of the Slater line for these atoms.  $C_1 = 0.3$  and  $C_2 = 0.1$  were guessed to be reasonable for Si and were used in the refinement.  $C_1 = 0.2, 0.4$  and  $C_2 = 0.1$  gave nearly as good results;  $C_1 = 0.6, C_2 = 0.1$  and  $C_1 = C_2 = 0$  led to significantly worse results.

The final parameter values (e.s.d.'s in parentheses) are:  $B = 0.4700$  (15)  $\text{\AA}^2$ ;  $q(\text{Si}) = 1.12$  (12) positive-charge units;  $V_{11} = 0.256$  (13),  $V_{33} = 0.174$  (14)  $\text{\AA}^2$ . From (1) we find  $q(\text{bond}) = 0.56$  e, which is larger than the value of HKKK, 0.45 e. On the other hand, HKKK's (isotropic) smearing tensor is smaller,  $V_{ii} = 0.164$   $\text{\AA}^2$ , which matches the difference in  $q$ . Thus, according to our calculation, more charge is transferred into the bond region and is more strongly smeared out. Moreover, the smearing is anisotropic,  $V_{11} > V_{33}$ , i.e. the charge is more strongly smeared out perpendicular to than along the bond. This result for silicon is in qualitative agreement with the interpretation by Brill (1960) of the (comparatively inaccurate) experimental data for diamond, and with the theoretical calculation by Ewald & Hönl (1936*a,b*), also for diamond.

### Comparison of the refinements of various density models

In order to demonstrate the appropriateness of our density model in matching the X-ray data, we present  $R$  and goodness-of-fit values for our and several other models in Table 2. These models are: the free-atom model, one model of the Dawson (1967) type from AH,

four multipole models of PMM, and one multipole model of HC. In this comparison we have to refer respectively to the same groups of reflections which were used in the refinements. We denote the groups by the numbers of the reflections: 15 = Mo  $K\alpha$  room-temperature data of AH, 17 = 15 plus the 222, 442 reflections, 21 = 17 plus the four HKKK reflections of Table 1. The results are given in Table 2, and we conclude:

(1) The improvement in fitting the data is significant for all bond-density models relative to the free-atom model (on the  $\alpha = 0.005$  level).

(2) Our four-parameter model yields much better figures in Table 2 than the two five-parameter multipole models of PMM, and slightly better figures than the five-parameter multipole model of HC.\*

(3) The eight-parameter models of PMM give about equally good values for the goodness-of-fit as our model, but better  $R$  values. However, with the value of Hamilton (1965),  $\chi^2(4, 7, 0.005) = 2.60$ , the improvement in  $R$  is not significant on the  $\alpha = 0.005$  level. For the model PMM3*a* it becomes significant for  $\alpha = 0.030$ , for the model PMM3*b* for  $\alpha = 0.010$ . Thus, it could be that, with the eight-parameter multipole models of PMM, a physically better description is obtained, but this does not appear to be highly probable.

Thus, we conclude that our model compares well with the multipole models of about the same number of parameters, and gives an adequate description of the density distribution in the crystal, at least for the purpose of fitting the X-ray data. We believe that this type of model is also suited to representing the density distribution in molecular crystals. First results were reported for decaborane and cyanuric acid (Dietrich & Scheringer, 1978, 1979), but there a somewhat different and less effective description of the spherical atomic cores was used.

\*  $R$  for the three-parameter model of AH with data set 15 (0.14%) appears to be abnormally low. Dawson (1975), in his review [Table 10, column  $f_{\text{mod}}(3''4'')$ ], does not confirm this value; according to Dawson it is  $>0.31\%$ .

Table 2.  $R$  (%) and goodness-of-fit values obtained in the refinements with various density models

PMM1, PMM2, PMM3*a*, PMM3*b* denote the models used by PMM, Tables 1, 2, 3*a*, 3*b*, respectively. FAM denotes the free-atom model with  $B = 4700$   $\text{\AA}^2$ . The numbers in brackets denote the number of parameters used, where  $B$  is included.  $R = 100 \sum |\Delta F| / \sum F_o$ ,  $\text{GoF} = [\sum w|\Delta F|^2 / (n - p)]^{1/2}$ .

	Data set	FAM (1)	AH (3)	PMM1 (5)	PMM2 (5)	PMM3 <i>a</i> (8)	PMM3 <i>b</i> (8)	HC (5)	Present work (4)
$R$	15	0.67	0.14	0.53	0.28	0.05	0.06	0.14	0.12
	17	0.94						0.16	0.13
	21	0.98						0.34	0.30
GoF	15	14.0		6.5	4.3	0.69	0.73	1.9	1.4
	17	15.9						1.9	1.3
	21	14.2						1.7	1.2

### The bond peak in the deformation density

We have already stated that, with the data sets 15 and 21, bond peaks of very different heights ( $0.13$  and  $0.29$   $e \text{ \AA}^{-3}$ , respectively) were obtained. In the following we shall show that the four HKKK reflections in the data set 21 cause an error in the peak height because they were not measured accurately enough. For these four reflections  $\sigma(F_o)$  is about one order larger [ $\sigma(F_o) \simeq 0.01F$ ] than for the AH reflections [ $\sigma(F_o) \simeq 0.001F$ ]. From Table 1 we infer that the four HKKK  $F_o$ 's deviate more from the  $F_c$ 's of both the bond model and the free-atom model than do the  $F_c$ 's for these two models from each other. Hence, it is impossible to distinguish between the two models by means of the four HKKK reflections. This also becomes evident when we compare the  $F_o - F_c$  maps with the deformation densities. In the  $F_o - F_c$  map with data set 17 (Fig. 2) we have an error level of  $0.02 e \text{ \AA}^{-3}$ , in the map with data set 21 (Fig. 3) an error level of  $0.08 e \text{ \AA}^{-3}$ . In

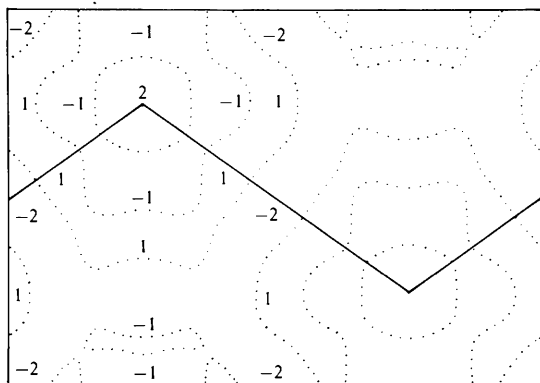


Fig. 2. Difference density calculated with coefficients  $F_o - F_c$  (bond model) from data set 17. Between the zero lines, fluctuations smaller than  $0.025 e \text{ \AA}^{-3}$  occur; these are indicated by numbers ( $\times 100$ ). Otherwise as Fig. 1.

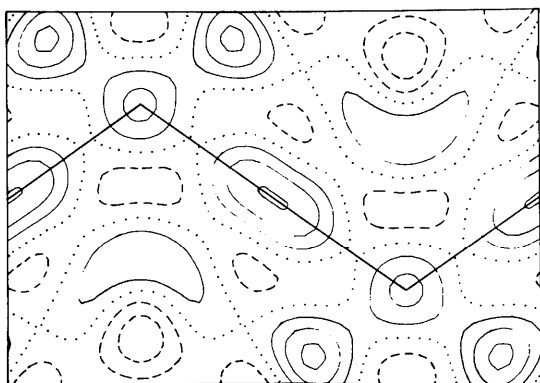


Fig. 3. Difference density calculated with coefficients  $F_o - F_c$  (bond model) from data set 21. Otherwise as Fig. 1.

the deformation density with data set 17 (Fig. 1) we have a bond peak of  $0.20 e \text{ \AA}^{-3}$ , with data set 21 a peak of  $0.29 e \text{ \AA}^{-3}$ . Thus the error level for data set 21 ( $0.08 e \text{ \AA}^{-3}$ ) is about as large as the increase of the peak height ( $0.09 e \text{ \AA}^{-3}$ ). Similarly,  $R$  increases much more in the transition from data set 17 ( $0.13\%$ ) to data set 21 ( $0.30\%$ ) than one would expect with the inclusion of only four additional data. The same trend is observed for the HC model, Table 2. The error in the HKKK intensities need not be of a systematic nature, since for three reflections  $|F_o - F_c$  (bond model)  $< \sigma(F_o)$ ; only for the 551 reflection  $|F_o - F_c| > \sigma(F_o)$ . This conclusion is also confirmed by a normal probability plot for data set 21, see Fig. 4 [the points represent weighted pairs of  $F_o, F_c$  (bonding model)]. The points for the four HKKK reflections are encircled. Only the 551 reflection lies on the upper right corner of the plot; the other three HKKK reflections fit into the central part well. Thus the plot for data set 21 is as good as that for data set 17 (which is not given here; it looks quite similar to the remainder of the plot for data set 21).

To exclude the possibility that the bond peak for data set 17 is heavily reduced by series termination, we assume that our bond model describes the density distribution in the bond region essentially correctly, and then investigate the effect of possible series-termination errors with our model. Firstly, we calculate structure factors for data sets 17 and 21 from the models and the corresponding deformation densities  $\rho$  (bond model) -  $\rho$  (free-atom model). For both sets of structure factors the bond peak is  $0.22 e \text{ \AA}^{-3}$  high. Then we calculate an

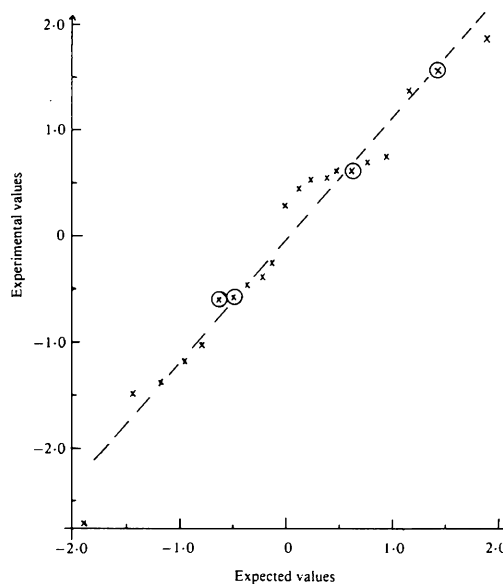


Fig. 4. Normal probability plot  $|F_o, F_c$  (bonding model)| for data set 21. The four HKKK reflections are encircled.

additional 90 structure factors up to the limit of  $\sin \theta/\lambda = 1.50 \text{ \AA}^{-1}$  and the corresponding deformation density. Its bond peak is  $0.24 \text{ e \AA}^{-3}$  high. Hence, we can conclude that an increase of the bond peak from  $0.20$  to  $0.29 \text{ e \AA}^{-3}$  is highly improbable by inclusion of a few accurately measured data (beyond the data set 17) in the Fourier series.

If we assume  $0.20 \text{ e \AA}^{-3}$  to be the nearly correct value for the peak height in the deformation density, then YC's valence density should also be reduced by about  $0.09 \text{ e \AA}^{-3}$  at the centre of the bond; *i.e.* instead of  $0.69 \text{ e \AA}^{-3}$  it will now be  $0.60 \text{ e \AA}^{-3}$ . This reduction does not impair the general agreement with the theoretical valence density of  $0.65 \text{ e \AA}^{-3}$  (as quoted by YC), but the deviation now is in the opposite direction.

The elimination of the thermal smearing in our model hardly changes the bond density. Structure factors calculated with  $B = 0$  in (2) yield a static deformation density with a bond peak of the same height ( $0.22 \text{ e \AA}^{-3}$ ) as in the dynamic deformation density. This general result was also obtained by YC, but with a different mathematical procedure.

We cannot confirm the error calculated by YC in the deformation density for data set 21,  $\sigma = 0.007 \text{ e \AA}^{-3}$ , based on the  $\sigma(F_o)$ 's. Instead we calculate  $\sigma = 0.036 \text{ e \AA}^{-3}$  which fits much better to the  $F_o - F_c$  map shown in Fig. 3 where the maximum-error level is  $0.08 \text{ e \AA}^{-3}$ . For data set 17, however, we calculate  $\sigma(\Delta\rho) = 0.009 \text{ e \AA}^{-3}$  which fits well to the maximum-error level of  $0.02 \text{ e \AA}^{-3}$  of the  $F_o - F_c$  map shown in Fig. 2.

If we wish to determine the (difference) density in the Si-Si bond with an accuracy of  $\delta = 0.02 \text{ e \AA}^{-3}$  and if we assume an average density of  $20 \text{ e \AA}^{-3}$  in the Si core, we are faced with a ratio of  $\delta/\rho = 10^{-3}$ . The four HKKK reflections, with  $\sigma(F_o)/F \simeq 10^{-2}$ , do not have the necessary accuracy. Hence, with silicon, inclusion of a few less accurately determined structure factors in the Fourier synthesis has a disastrous effect, and lowers considerably the standard which has been obtained with the remaining data.

I thank Dr N. K. Hansen, Berlin, for sending a list of structure factors from which the figures in Table 2 for the HC model were calculated, and Dr A. Kutoglu, Marburg, for his help in using the Fourier program of Finger & Prince (1975).

### References

- ALDRED, P. J. E. & HART, M. (1973). *Proc. R. Soc. London Ser. A*, **332**, 223–238, 239–254.
- BRILL, R. (1959). *Z. Elektrochem.* **63**, 1088–1091.
- BRILL, R. (1960). *Acta Cryst.* **13**, 275–276.
- COPPENS, P. (1977). *Isr. J. Chem.* **16**, 159–162.
- COPPENS, P., GURU ROW, T. N., LEUNG, P., STEVENS, E. D., BECKER, P. J. & YANG, Y. W. (1979). *Acta Cryst.* **A35**, 63–72.
- DAWSON, B. (1967). *Proc. R. Soc. London Ser. A*, **298**, 379–394.
- DAWSON, B. (1975). *Advances in Structure Research by Diffraction Methods*, Vol. 6. Braunschweig: Vieweg.
- DE MARCO, J. J. & WEISS, R. J. (1965). *Phys. Rev. A*, **137**, 1869–1871.
- DIETRICH, H. & SCHERINGER, C. (1978). *Acta Cryst.* **B34**, 54–63.
- DIETRICH, H. & SCHERINGER, C. (1979). *Acta Cryst.* **B35**, 1191–1197.
- EWALD, P. P. & HÖNL, H. (1936a). *Ann. Phys. (Leipzig)*, [5], **25**, 281–308.
- EWALD, P. P. & HÖNL, H. (1936b). *Ann. Phys. (Leipzig)*, [5], **26**, 673–696.
- FINGER, L. W. & PRINCE, E. (1975). *Natl. Bur. Stand. (U.S.) Note* 854.
- FUJIMOTO, I. (1974). *Phys. Rev. B*, **9**, 591–599.
- GÖTTLICHER, S. & WÖLFEL, E. (1959). *Z. Elektrochem.* **63**, 891–901.
- HAMILTON, W. C. (1965). *Acta Cryst.* **18**, 502–510.
- HANSEN, N. K. & COPPENS, P. (1978). *Acta Cryst.* **A34**, 909–921.
- HATTORI, H., KURIYAMA, H., KATAGAWA, T. & KATO, N. (1965). *J. Phys. Soc. Jpn.* **20**, 988–996.
- HIRSHFELD, F. L. (1971). *Acta Cryst.* **B27**, 769–781.
- International Tables for X-ray Crystallography* (1974). Birmingham: Kynoch Press.
- MCCONNELL, J. F. & SANGER, P. L. (1970). *Acta Cryst.* **A26**, 83–93.
- PRICE, P. F., MASLEN, E. N. & MAIR, S. L. (1978). *Acta Cryst.* **A34**, 183–193.
- ROBERTO, J. B. & BATTERMAN, B. W. (1970). *Phys. Rev. B*, **2**, 3220–3226.
- SCHERINGER, C. (1977). *Acta Cryst.* **A33**, 426–429, 430–433.
- SCHERINGER, C. (1979). *Acta Cryst.* **A35**, 700.
- TRUCANO, P. & BATTERMAN, B. W. (1972). *Phys. Rev. B*, **6**, 3659–3666.
- WAGENFELD, H., KÜHN, J. & GUTTMAN, A. J. (1973). Abstracts, First European Crystallography Conference, Bordeaux.
- YANG, Y. W. & COPPENS, P. (1974). *Solid State Commun.* **15**, 1555–1559.